Supporting information for:

Decomposition mechanism of Anisole on Pt(111). Combining single crystal experiments and first principle calculations.

Romain Réocreux,[‡] Cherif A. Ould Hamou,[†,§] Carine Michel,[‡] Javier B. Giorgi,[†,‖,*] Philippe Sautet[‡,&,*]

[‡] Univ Lyon, Ens de Lyon, CNRS UMR 5182, Université Claude Bernard Lyon 1, Laboratoire de Chimie, F-69342, Lyon, France

[†] Centre for Catalysis Research and Innovation, [§] Department of Physics, [‖] Department of Chemistry and Biomolecular Sciences, University of Ottawa, 10 Marie Curie Pvt., Ottawa, Ontario, Canada. K1N 6N5.

[&] Department of Chemical and Biomolecular engineering, University of California, Los Angeles, Los Angeles, CA 90095, United States

Corresponding authors:
JBG email: Javier.giorgi@uottawa.ca
PS email: Philippe.sautet@ens-lyon.fr

Coverage Calibration with C 1s XPS

The C 1s XPS signal was monitored for different exposures of anisole on Pt(111) at 115K. The C1s area reaches a plateau which correspond to the saturation of the monolayer. Coverage calibration was achieved by comparison with CO saturation coverage at room temperature. Dashed line in figure S1 indicates the area of the C 1s peak from a CO coverage surface which is known to correspond to one CO molecule per two Pt atoms on the surface. That is, C/Pt atomic ratio of 0.5. Upon monolayer coverage of anisole, a C/Pt ratio of 0.7 is achieved which corresponds to one molecule of anisole (7 carbon atoms) for each 10 Pt atoms on the surface.

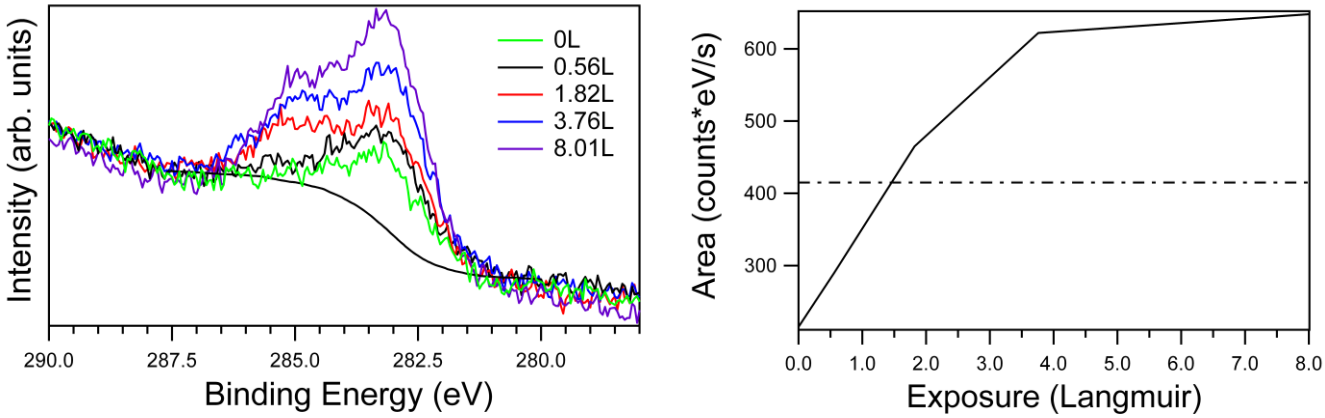

Figure S1. C1s spectra and corresponding integrated area after several exposures of anisole at 115K on Pt(111). The C1s starts reaching a plateau around 2.8 Langmuir corresponding to the saturation of the 1st layer of anisole on the platinum surface. Dash line correspond to calibration point from CO adsorption on Pt(111).

Oxygen XPS

The O 1s XPS signal was monitored for all measurements. Disappearance of the oxygen signal matches the disappearance of the C 1s species assigned to oxygen bound carbons species (C-O labeled peaks).

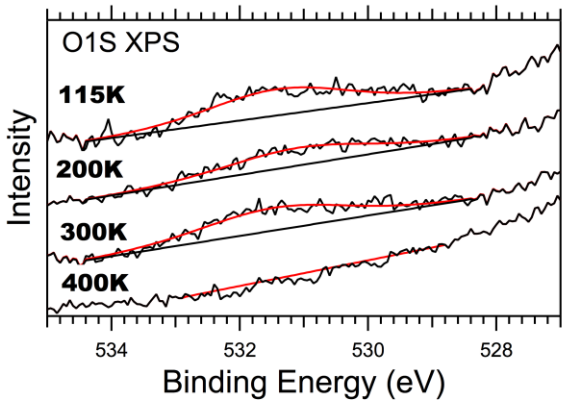

Figure S2. XPS spectra for the O 1s peak acquired at different temperature for 0.5ML of anisole deposited at 115K.

Correction of TPD signal due to fragmentation of species in the mass spectrometer

Because all organic species fragment during the ionization process in the mass spectrometer, it is necessary to identify the fraction of signal at specific mass to charge intensities corresponding to species desorbing from the surface versus those that arise from fragmentation. To perform the correction, appropriate parent molecules (for example anisole) are dosed into the chamber in the gas phase and the mass spectrum is obtained to identify the corresponding fragmentation pattern specific to the instrument (Figure S3a). In this case the ratio of intensities of masses 78/108 was determined as 2.6. Since we monitor TPD of the masses simultaneously, this allows us to quantify the fraction of m/z=78 corresponding to fragmentation of anisole in the QMS and subtract it from the overall benzene signal. The result is the identification of benzene arising from surface desorption (Figure S3b).

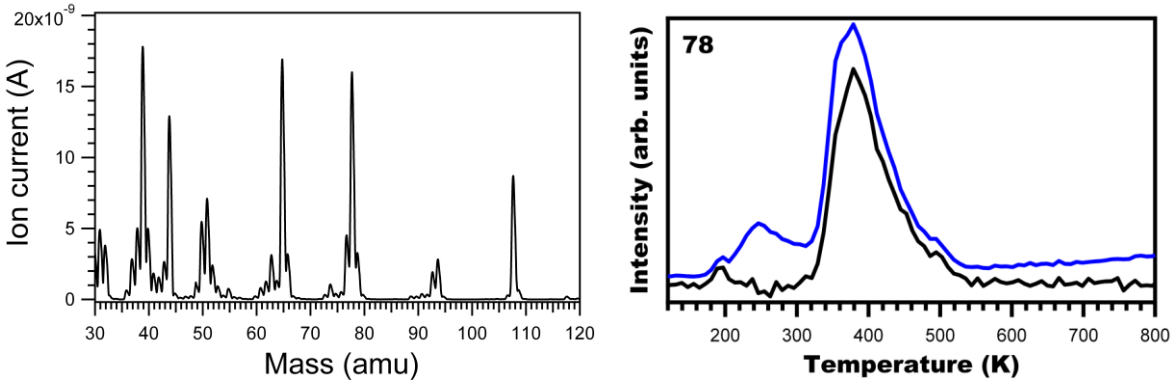

Figure S3. a) Mass spectrum of gas phase anisole illustrating the instrument specific fragmentation pattern. b) TPD spectra after multilayer exposure of anisole at 115K on Pt(111) using a linear temperature ramp of 7 K/s. The blue line corresponds to benzene raw data as measured by the mass-spectrometer. The black line corresponds to benzene produced from the surface (data obtained after the subtraction of contribution of the gas phase fragmentation pattern of anisole in the mass spectrometer).

XPS vs TPD consistency.

To justify that the TPD analysis is consistent with the XPS interpretation of the experiment we calculated, from the TPD-determined frequency factors and activation energies, the expected half-lives (in hour) as a function of temperature. The processes can be considered as kinetically blocked when the half-lives are

greater than an hour (blue values) and kinetically possible when the half-lives are much smaller than an hour. From this, we can calculate the expected temperature at which a process will happen during the XPS measurement that lasts one hour. The half-lives presented here were calculated assuming a first-order Arrhenian process with the associated TPD-determined parameters.

	Anisole decomposition	physiorption PhOMe	chemisorption PhOMe	CO desorption
frequency (s-1)	1.70E+14	5.40E+16	2.40E+17	8.30E+14
TPD barrier (kJ/mol)	89	83	121	137
T (K)	half life (hour) for a 1st order process			
100	5.08E+26	8.10E+22	1.29E+42	8.50E+52
115	4.38E+20	1.79E+17	7.35E+33	3.94E+43
150	1.62E+11	2.86E+08	1.10E+21	1.19E+29
200	2.89E+03	1.70E+01	3.22E+10	1.40E+17
210	2.26E+02	1.58E+00	1.01E+09	2.78E+15
220	1.54E+03	1.82E-01	4.31E+07	7.84E+13
230	1.85E+02	2.53E-02	2.43E+06	3.02E+12
240	2.66E+01	4.14E-03	1.74E+05	1.53E+11
250	4.47E+00	7.85E-04	1.54E+04	9.80E+09
260	8.61E-01	1.69E-04	1.64E+03	7.76E+08
270	1.87E-01	4.07E-05	2.06E+02	7.42E+07
280	4.55E-02	1.09E-05	3.01E+01	8.40E+06
290	1.22E-02	3.18E-06	5.01E+00	1.10E+06
300	3.56E-03	1.01E-06	9.40E-01	1.66E+05
310	1.12E-03	3.45E-07	1.97E-01	2.82E+04
320	3.82E-04	1.26E-07	4.53E-02	5.36E+03
330	1.39E-04	4.90E-08	1.14E-02	1.13E+03
340	5.34E-05	2.01E-08	3.12E-03	2.59E+02
350	2.17E-05	8.70E-09	9.19E-04	6.49E+01
360	9.29E-06	3.94E-09	2.89E-04	1.76E+01
370	4.16E-06	1.86E-09	9.71E-05	5.09E+00
380	1.94E-06	9.16E-10	3.45E-05	1.58E+00
390	9.43E-07	4.67E-10	1.29E-05	5.19E-01
400	4.75E-07	2.46E-10	5.08E-06	1.80E-01
450	2.43E-08	1.54E-11	8.92E-08	1.86E-03
500	2.25E-09	1.67E-12	3.51E-09	4.77E-05
550	4.77E-09	2.72E-13	2.49E-10	2.38E-06
600	8.64E-10	6.00E-14	2.75E-11	1.96E-07
XPS temperature (K)	270	220	310	390

Table S1: Half-lives of 4 given processes, namely anisole decomposition, physisorbed anisole desorption and chemisorbed anisole desorption, and carbon monoxide desorption. The half-lives, calculated from TPD-determined parameters, are given as a function of temperature.

DFT predicted infrared spectrum of phenoxy PhO

The RAIRS simulated spectrum was generated from a VASP frequency calculation by computing the contribution of the dipole moment along the direction perpendicular to the surface (RAIRS selection rule) at

each displacement. The associated matrix was diagonalized and the intensity of each normal mode was determined using the squared variation of the dipole moment.

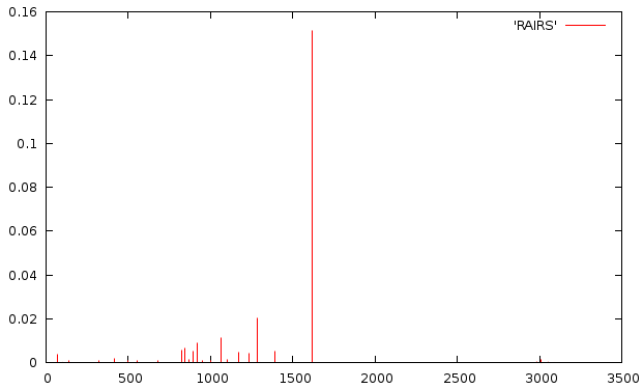

Figure S4: DFT predicted infrared spectrum of phenoxy PhO.

The strong peak at 1616 cm^{-1} corresponds to the stretching mode of the C-O bond. The value of the wave number is typical for a carbonyl function and matches with the experimentally observed cyclohexadienyl structure of "phenoxy" on Pt(111).

Reaction network for phenoxy decomposition.

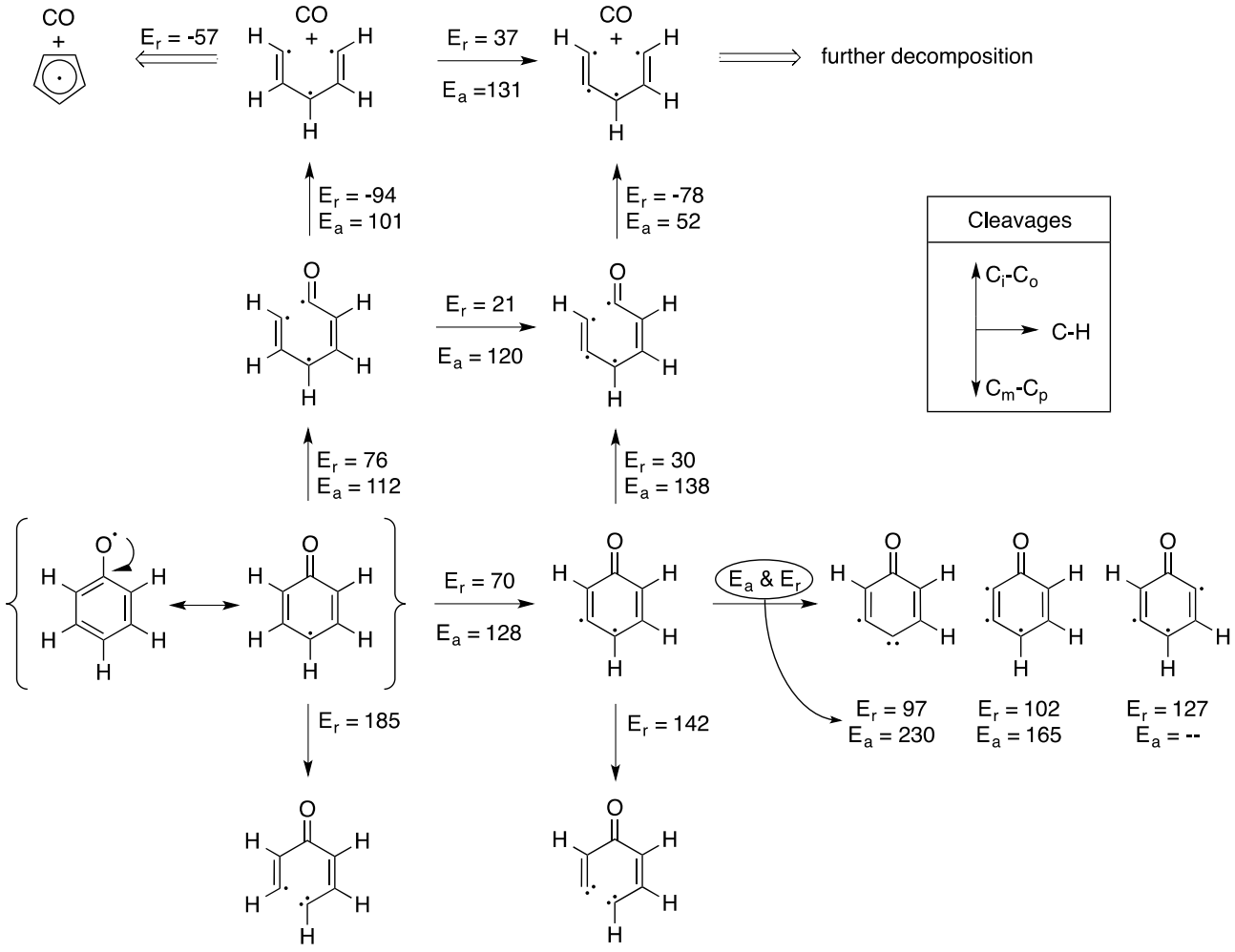

Figure S5. Reaction network of phenoxy decarbonylation to carbonaceous species. Downward, upward and rightward arrows are associated to the meta-para C-C, ipso-para C-C and aromatic C-H cleavages respectively. E_r and E_a stand for reaction and activation energies respectively. The energies are given in kJ/mol and are not ZPE-corrected.

Kinetic analysis of the DFT data.

In a TPD experiment, two time-scales have to be compared: the one imposed by the operator through the choice of the temperature ramp (here $\beta = 7\ K/s$) and the ones that are specific to the reactivity of the chemicals. If the reaction time is smaller than the TPD time-scale T/β, then one can observe the reaction happening. Otherwise, the reaction is to slow to be observed within the time of the TPD experiment. In this work we considered the 1% conversion time $\tau_{1\%}$ since only a small fractions of the initially adsorbed species yield desoring products. A reaction is therefore considered to happen when:

$$\tau_{1\%} < \frac{T}{\beta}$$

Using Eyring's equation for a 1st order process:

$$\tau_{1\%} = \frac{-\ln(0.99)\,h}{k_B T} \exp\left(+\frac{\Delta F^{\ddagger}}{RT}\right) < \frac{T}{\beta}$$

One can then extract the limit we considered in the main text of the article:

$$\Delta F^{\ddagger} \simeq RT ln\left(\frac{k_B T^2}{-\ln(0.99)\,h\beta}\right)$$

Intermediates and transition states of the routes to benzene and phenol

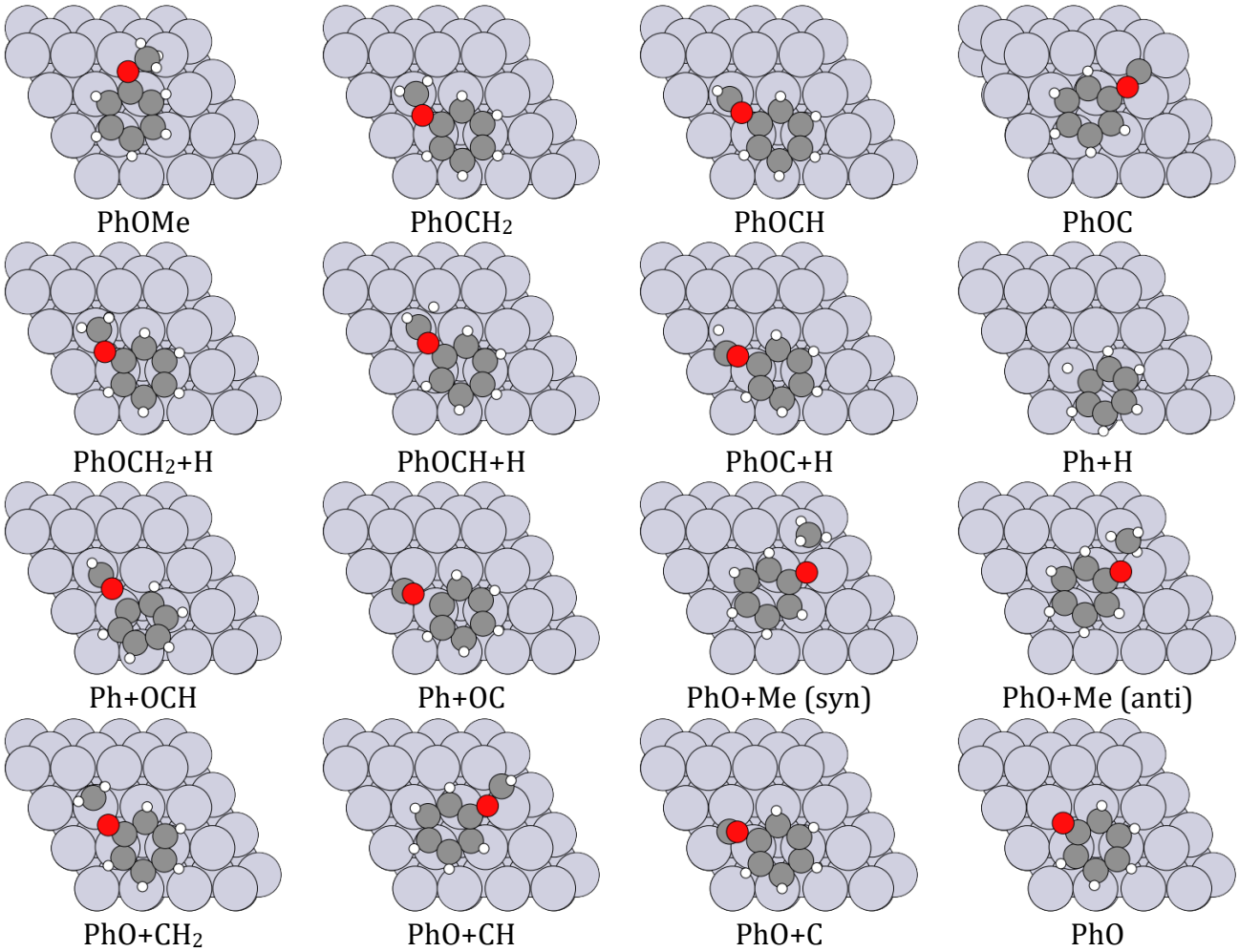

Figure S6. Structures of the intermediates and transition states associated to the benzene and phenol routes.

Intermediates and transitions states of the routes to phenoxy fragmentation.
The structures appear here in the same order as in Figure 11 (main article).

Mechanism #1

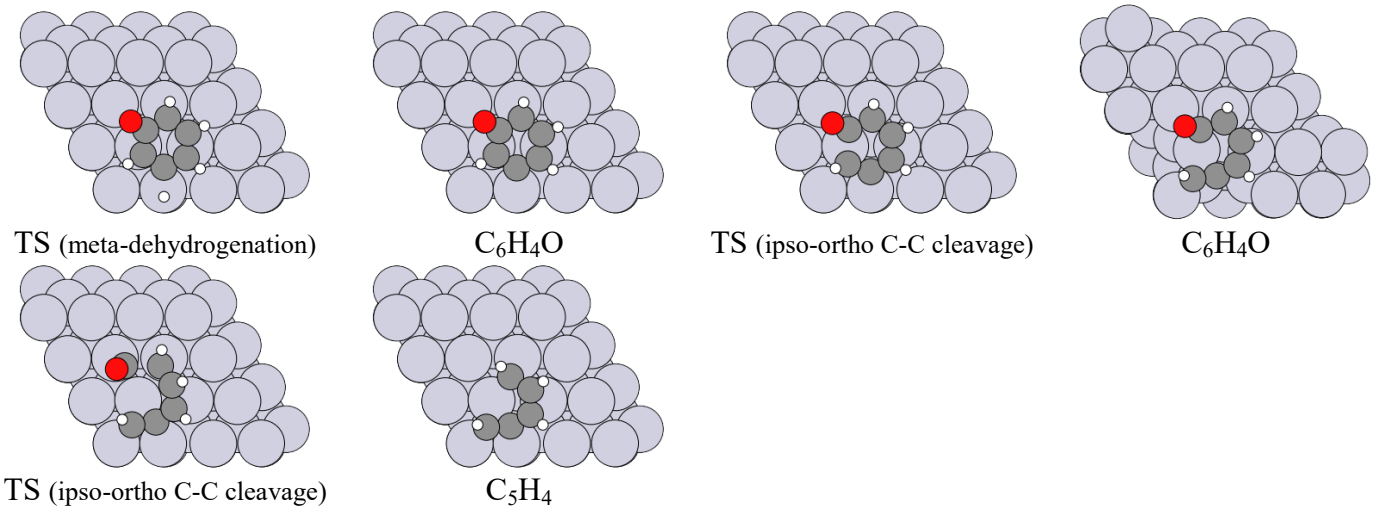

Figure S7. Structures of the intermediates and transition states associated to the 1st mechanism of the fragmentation of phenoxy.

Mechanism #2

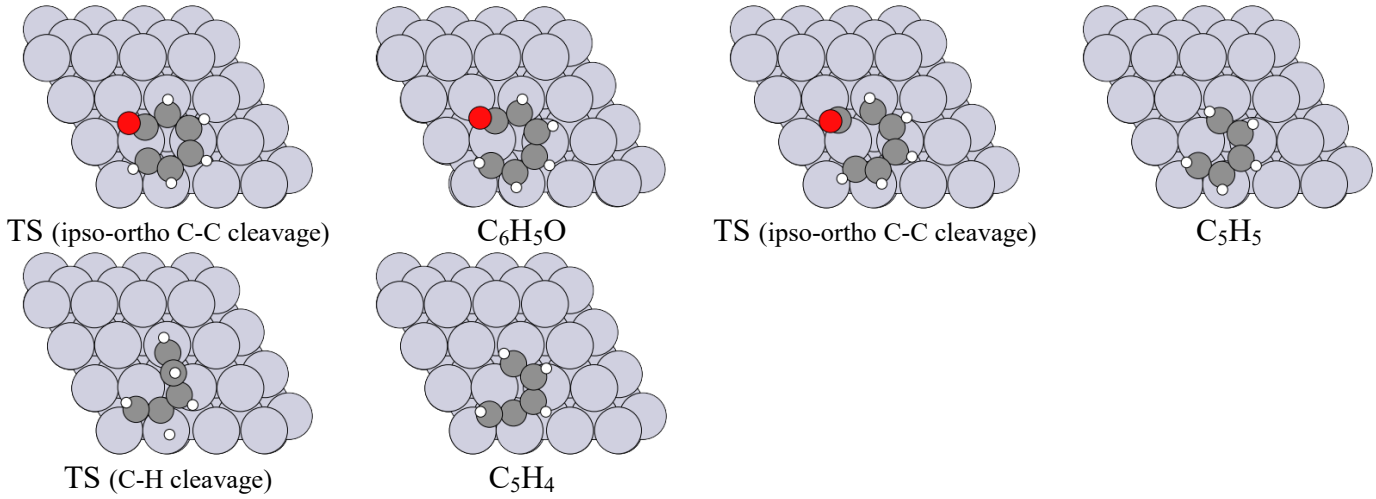

Figure S8. Structures of the intermediates and transition states associated to the 2nd mechanism of the fragmentation of phenoxy.